Numerical Simulations of Nitric Oxide (NO) Formation in Methane, Methanol and Methyl Formate in different Flow Configurations

P. N. Kioni, J. K. Tanui, and A. Gitahi

Abstract—**Methane/air, methanol /air and methyl formate /air have been numerically simulated in three different flow configurations: homogeneous system; freely propagating flame; and diffusion flame. These simulations have been done with an aim of establishing the influence of fuel oxygenation on generation of pollutant. Various chemical kinetic mechanisms have been employed and extensively tested so as to ensure validity of the results. For each of the three configurations, a comparison of temperature, NO and its immediate dominant precursor species (CH and N) concentration profiles in the three fuels have been done. It has been established that, under the different flow configurations considered, CH_4 has high amount of total NO present in the flame region as compared to the oxygenated fuels (CH_3OH and CH_3OCHO). The temperatures attained in freely propagating and diffusion flames are relatively low (approximately ≤ 2000 K). This temperature favours prompt-NO formation, and therefore, a significant difference of the amount of NO (one order of magnitude higher) is observed in CH_4 as compared to oxygenated fuels due to low values of CH and N observed in these fuels (CH_3OH and CH_3OCHO). High flame temperatures (approximately 2900 K) due to high initial temperatures are observed in the homogeneous system. Therefore, in homogeneous system it was observed that the amount of NO produced by the three fuels is within the same order of magnitude due to availability of the O atoms and nitrogen molecules (important species in thermal NO mechanism (Zel'dovich mechanism)).**

Index Terms—**Methane, methanol, methyl formate, prompt NO, thermal NO.**

I. Introduction

The understanding of chemical pathways formation for NO in a fuel oxidation is very important in determining the reduction techniques to be employed in a combustion system. NO in a flame is formed mostly through thermal NO (Zel'dovich mechanism) and prompt-NO. Thermal NO is formed at high temperature flame zone, whereas prompt-NO is formed at low temperature flame zone. NO formations in different fuels have been the subject of many studies. NO formations in methane as well as methanol have been well understood [1]-[6]. However, nitric oxide formation in methyl formate has not been studied widely. We recently reported [7], [8] on NO formation in methyl formate in a homogeneous system and a freely propagating flame. The aim of this paper is to investigate the influence of different flow configurations: homogeneous system; freely propagating flame; and diffusion flame, on generation of NO in a methyl formate.

The chemical kinetics of a real fuel, which consists of large carbon chain, is complex. For instance, a typical biodiesel fuel has C14-C18 fatty acid methyl esters: methyl palmitate, methyl stearate, methyl oleate, methyl linoleate and methyl linolenate in different compositions. However, several kinetics models for both small-chain and long-chain methyl esters have been developed. These include: detailed chemical kinetic mechanism for methyl formate [9]-[11], methyl butanoate [10], methyl hexanoate and methyl heptanoate [12], methyl-5-decenoate and methyl-9-decenoate [13], methyl stearate and methyl oleate [14]. Recently, Westbrook et al. [15] developed a mechanism for the five major components of soy biodiesel and rapeseed biodiesel fuel. These mechanisms usually have numerous chemical species taking part in enormous reactions, for instance, Naik et al. [14] chemical reaction mechanism has 3500 species taking part in 17,000 chemical reactions. These detailed mechanisms can only be used to model fuels in zero dimensional homogenous transient system. It is impractical to implement them in one and two dimensional flame codes due to computational limitation. However, a skeletal (reduced) mechanism can be derived from the detailed mechanism, such as those used by Sarathy et al. [16], and Valeri and Junfeng [17].

The kinetics models described in the preceding paragraph have been used to study several aspects of methyl esters combustion: intermediate species production; ignition and extinction; the effects of saturation; the effects of molecular structure, et cetera. However, kinetics models for NO_x formation in esters do not exist in literature.

NO concentration profiles for methyl formate in all configurations studied in this paper have been compared to those of methane/air and methanol/air flames which are well understood. Various chemical kinetic mechanisms have been employed for the different fuels. Methane and methanol flames are computed using GRI-Mech 3.0 reaction mechanism [18], while methyl formate flame is computed by combining the Dooley et al. [19] oxidation mechanism with the Leeds NO_x oxidation mechanism [20], GRI-Mech 3.0 reaction mechanism has been validated and tested in previous investigations: [5], [21]. Dooley et al. [19] oxidation mechanism has also been validated in a wide range of conditions, viz, a variable pressure flow reactor, shock tube facility, outwardly propagating flames and burner stabilized

Manuscript received December 18, 2012; revised January 24, 2013. This work was supported by Dedan Kimathi University of Technology.

P. N. Kioni and J. K. Tanui are with the Department of Mechanical Engineering, Dedan Kimathi University of Technology, Nyeri-Kenya (e-mail: ndirangukioni@yahoo.com, josetanui@gmail.com).

A. Gitahi is with the Department of Mechanical Engineering, Jomo Kenyatta University of Agriculture & Technology, Nairobi-Kenya (email: gitahi@eng.jkuat.ac.ke).

flames. Similarly, Leeds NO_x oxidation mechanism has been validated in flow reactors, perfectly stirred reactors and low pressure laminar flames by Hughes et al. [22].

II. Numerical Models

A. Homogeneous System

The system has been modeled as an adiabatic homogeneous mixture with constant internal energy and constant volume, which represent the experimental conditions behind a reflected shock in a shock tube apparatus. Methane/air, methanol/air, and methyl formate/air mixtures have been studied at constant volume of 200 cm^3, low pressure of 2.7 atm, and temperature of 1300 K. The governing equations for this configuration are single point transient (zero-dimensional time dependent), as derived in [23], are as follows:

$$\rho \frac{\partial Y_i}{\partial t} = w_i \quad i = 1, \dots, N, \tag{1}$$

$$\rho c_v \frac{\partial T}{\partial t} = -\sum_{i=1}^{N} u_i w_i + \frac{Q}{V}, \tag{2}$$

$$p = \rho RT \sum_{i=1}^{N} \left(\frac{Y_i}{W_i}\right). \tag{3}$$

Here, ρ is the density, t is the time, c_v is the specific heat capacity at constant volume, p is the pressure, R is the universal gas constant, T is the temperature, N is the total number of species, V is the reactor volume, Q is the rate at which heat is transferred across the reactor, while u_i, w_i, Y_i and W_i represent the internal energy, the rate of production by chemical reactions, the mass fraction and the molecular weight of species i, respectively.

B. Freely Propagating Flame

A laminar, one-dimensional premixed, freely propagating flame configuration as shown in Fig. 1 has been considered. The cold fuel-air mixture enters the computational domain through the left boundary, and hot combustion products exit the domain through the right boundary.

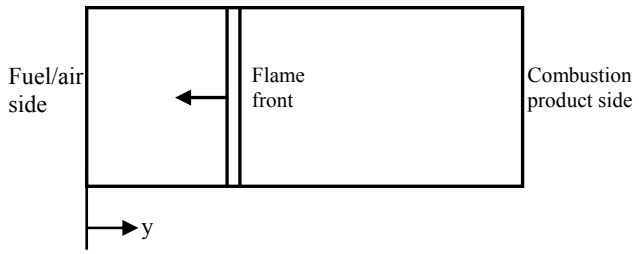

Fig. 1. Flow configuration for a freely propagating flame

This flame is assumed to be free from external disturbances which may be imposed by the presence of near-by walls and flame-anchoring devices. In addition, the thermodynamic part of the pressure is taken as spatially uniform, the effect of viscous dissipation and the body forces are neglected. Thus the governing equations, as derived in [23], are as follows:

$$\frac{\partial \rho}{\partial t} + \frac{1}{A}\frac{\partial}{\partial y}\left(\rho V_y A\right) = 0; \tag{4}$$

$$\rho\left(\frac{\partial Y_i}{\partial t} + V_y \frac{\partial Y_i}{\partial y}\right) = -\frac{1}{A}\frac{\partial}{\partial y}(\rho Y_i V_i A) + w_i \quad i = 1, \dots, \mathrm{N}, \tag{5}$$

$$\rho c_p \left(\frac{\partial T}{\partial t} + V_y \frac{\partial T}{\partial y}\right) = \frac{1}{A}\frac{\partial}{\partial y}\left(\lambda A \frac{\partial T}{\partial y}\right) - \frac{\partial T}{\partial y}\sum_{i=1}^{N} c_{pi}\rho Y_i V_i - \sum_{i=1}^{N} h_i w_i + \frac{dp}{dt} - \frac{1}{A}\frac{\partial}{\partial y}(q_R A) + A_s h_s (T - T_s), \tag{6}$$

$$p = \rho RT \sum_{\mathrm{i}=1}^{\mathrm{N}} \left(\frac{Y_i}{\mathrm{W_i}}\right). \tag{7}$$

Besides the quantities defined before, y is the spatial coordinate, A is the spatially variable cross sectional area, p is the pressure, V_y is the velocity in y direction, λ is the thermal conductivity, h_s is the heat transfer coefficient between gas and solid phase, q_R is the radiant heat flux, A_s is the local wetted surface area per unit void volume, T_s is the temperature at the solid surface, while V_i, h_i, and c_{pi} represent the diffusion velocity, the specific enthalpy, and the specific heat capacity at constant pressure of species i, respectively.

C. Diffusion Flame

The flow configuration considered is as shown in Fig. 2, with the fuel and air side positioned at left and right hand side, respectively. The temperature of both the fuel and air stream is taken as 300 K. The flames are computed at a constant pressure of 1 bar and a strain rate of 50 s^{-1}. At the fuel nozzle, pure fuel concentration (mole fraction of 1) is specified, while at the air nozzle, the mole fractions concentration of O_2 and N_2 are specified using the air standard composition.

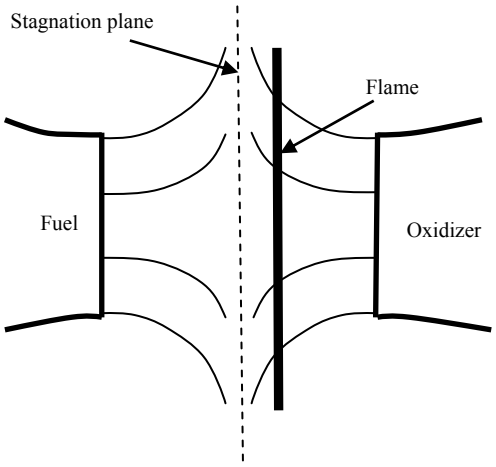

Fig. 2. Flow configuration for a diffusion flame

The flame is assumed to be embedded in a thin boundary-layer formed by stagnating flow; hence the computation requires the use of the boundary layer theory approximations. Though the flame is two-dimensional, under this assumption the equations of conservation reduced to one-dimensional forms. In addition, the thermodynamic part of the pressure is taken as spatially uniform, the effect of viscous dissipation, the Soret and Dufour, and the body forces are neglected. Thus the governing equations, as derived in [23] are as follows:

$$L_1(1) = 0, \tag{8}$$

$$L_1(G) = \frac{\partial}{\partial y}\left(\mu \frac{\partial G}{\partial y}\right) - \rho G^2 + P'(t), \quad (9)$$

$$c_p L_1(T) = \frac{\partial}{\partial y}\left(\lambda \frac{\partial T}{\partial y}\right) - \frac{\partial T}{\partial y}\sum_{i=1}^{N} c_{pi}\rho Y_i V_i$$

$$-\sum_{i=1}^{N} h_i w_i + \frac{dp}{dt} - \frac{\partial q_R}{\partial y}, \quad (10)$$

$$L_1(Y_i) = -\frac{\partial}{\partial y}(\rho Y_i V_i) + w_i \quad i = 1, \ldots, N. \quad (11)$$

Here L1 is the accumulative-convective operator given by

$$L_1(\Phi) = \frac{\partial(\rho\Phi)}{\partial t} + \frac{\partial(\rho V_y \Phi)}{\partial y} + \rho G \Phi, \quad (12)$$

Besides the quantities defined before, the function $G(y,t) = V_x/x$, Φ denotes the dependent variables and μ is the dynamic viscosity. The term in P' appearing in the momentum equation (9) represents a temporal forcing term defined by

$$P'(t) = \rho_f \left(\frac{da}{dt} + a(t^2)\right),$$

where a is the strain rate which is prescribed.

III. Numerical Solution Method

The flames are numerically simulated using the RUN1DL code in the software package [24]. Conservation equations are discretized with finite difference method. Both central and one-sided difference (upwind) schemes are adopted in the discretization of first-order derivatives, while central difference scheme is adopted for the second-order derivatives. For the case of upwind scheme applied to first-order derivatives, first-order accuracy is achieved. When second-order accurate central difference scheme is applied to a second-order derivative in a non-uniform grid, one order of accuracy is lost. Numerical accuracy is enhanced by having many grid points in the region of high gradient and having the grids points which are approximately equally spaced. This has been achieved by applying adaptive selection of grid point technique. Modified Newton method has been applied to the resulting nonlinear differential algebraic equations.

The thermodynamic properties (the frozen specific heat capacities at constant pressure of the pure species i, c_{pi}, the frozen specific heat capacity at constant pressure of the gas mixture, c_p, and the enthalpy, h_i, for pure species i) are calculated using polynomial curve fits of NASA type [25]. The transport properties required are the dynamic viscosity, μ and the thermal conductivity, λ, of the gas mixture, which are calculated using the method illustrated in [23].

IV. Results and Discussions

NO production in combustion system is mainly controlled by temperature. Maximum flame temperatures of approximately 1930 K - 1980 K (shown in Fig. 3) are observed for the three fuels in freely propagating flames. Under these temperatures, NO is produced mainly through prompt-NO. The maximum total NO produced in this flame type, as shown in Fig. 4, is to the order of 10^{-5} for CH_4 and 10^{-6} for CH_3OH and CH_3OCHO. In prompt NO, reaction: CH + N_2 = HCN + N is the determining step. A small amount of dominant immediate precursor species CH (Fig. 5) and subsequently N (Fig. 6) atoms in CH_3OH and CH_3OCHO explain the low values of NO concentration as compared to that for CH_4.

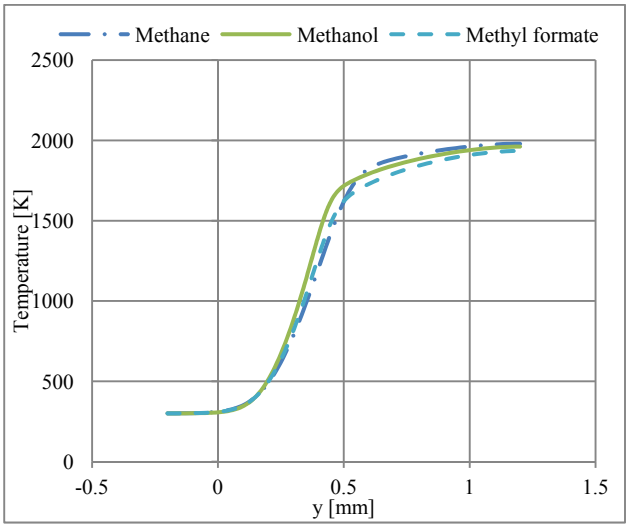

Fig. 3. Temperature profiles for methane, methanol and methyl formate/air freely propagating flames, Φ = 1

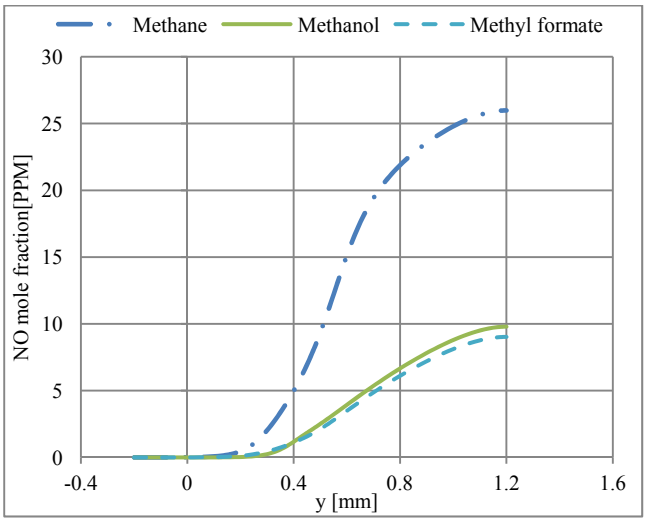

Fig. 4. NO concentration profiles for methane, methanol and methyl formate/air freely propagating flames

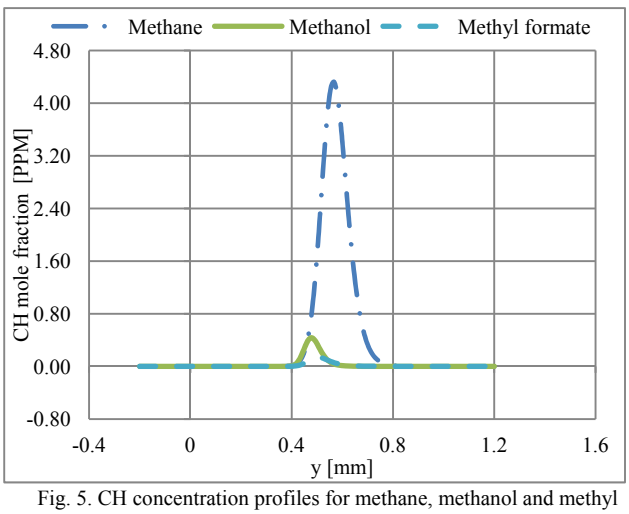

Fig. 5. CH concentration profiles for methane, methanol and methyl formate/air freely propagating flames

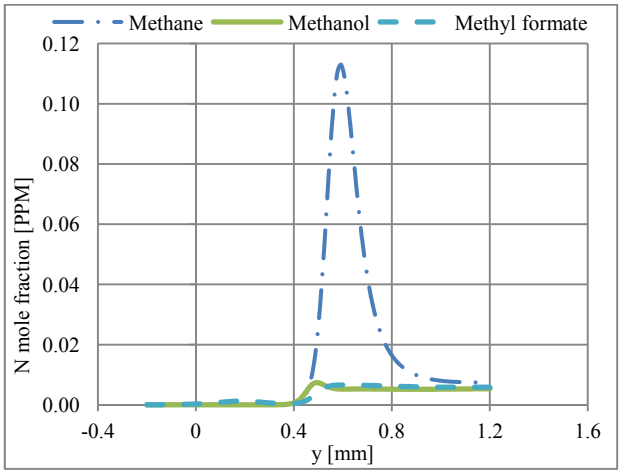

Fig. 6. N concentration profiles for methane, methanol and methyl formate/air freely propagating flames

Maximum flame temperatures of approximately 1960 K - 2050 K (shown in Fig. 7) are observed for the three fuels in diffusion flames. The maximum total NO produced in this flame type, shown in Fig. 8, is to the order of 10^{-4} for CH_4 and 10^{-5} for CH_3OH and CH_3OCHO. Just like in the freely propagating flames, the temperatures attained by diffusion flames favour the production of NO mainly through prompt-NO. With the small amount of CH (Fig. 9) and N (Fig. 10) atoms observed in CH_3OH and CH_3OCHO, the same argument applies as in freely propagating flames.

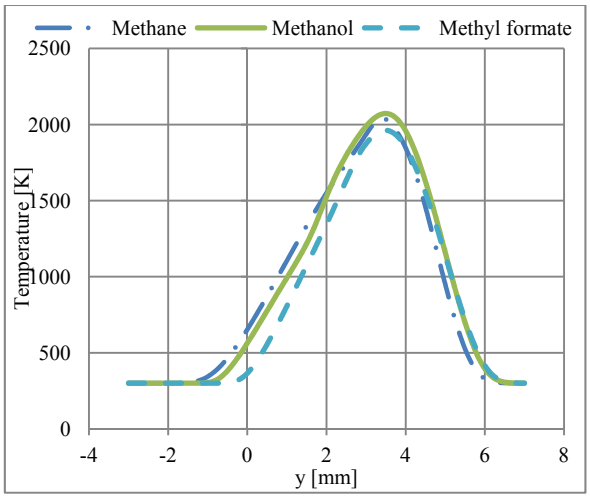

Fig. 7. Temperature profiles for methane, methanol and methyl formate/air diffusion flames

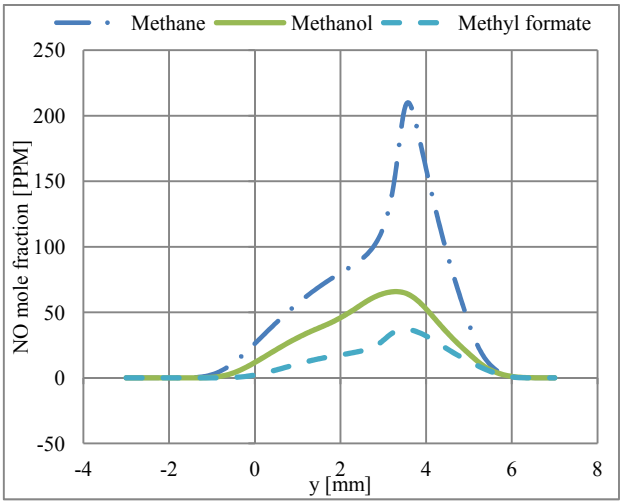

Fig. 8. NO concentration profiles for methane, methanol and methyl formate/air diffusion flames

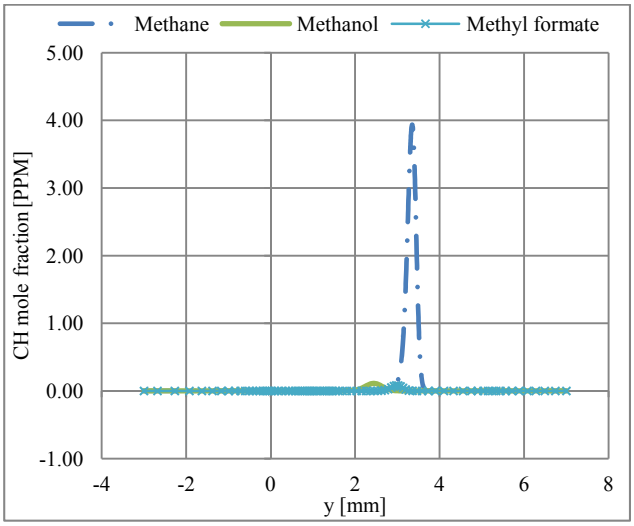

Fig. 9. CH concentration profiles for methane, methanol and methyl formate/air diffusion flames

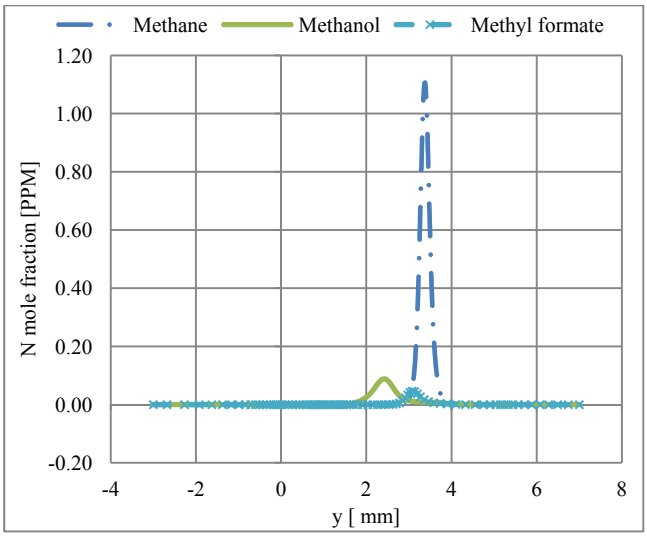

Fig. 10. N concentration profiles for methane, methanol and methyl formate/air diffusion flames

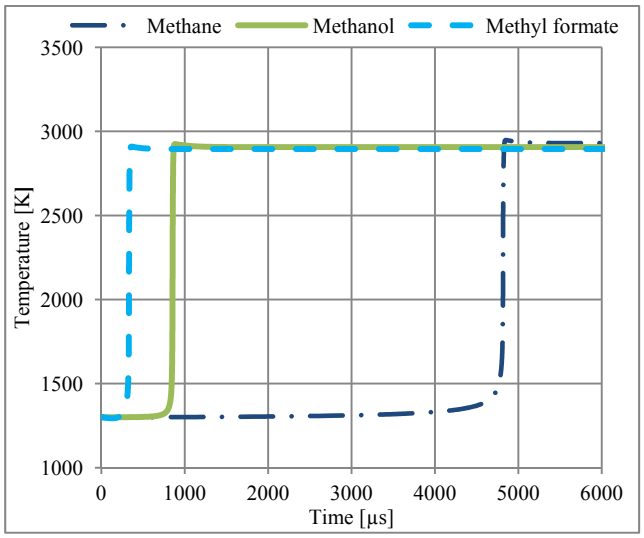

Fig. 11. Temperature profiles for methane, methanol and methyl formate/air homogeneous mixtures at temperature of 1300 K and pressure of 2.7 atm

In homogenous system, maximum flame temperatures of approximately 2900 K - 2930 K (shown in Fig. 11) are observed for the three fuels. The maximum total NO

produced in this flame type, shown in Fig. 12, is to the order of 10^{-2} for all fuels. Under these temperatures, thermal NO reaction by Zel'dovich mechanism is the dominating source of NO. The rate-limiting step in the Zel'dovich mechanism: $N_2 + O = NO + N$ is the decisive reaction for NO formation at high temperature. The availability of the O atoms and nitrogen molecules in all three fuels considered result in a similar amount of NO formed. The small difference in the production of NO is attributed to the different maximum temperatures attained by these mixtures and the prompt NO formation (as depicted in Fig. 13 and Fig. 14, where the prompt-NO precursor species CH and N, respectively, are significantly high for CH_4 as compared to CH_3OH and CH_3OCHO).

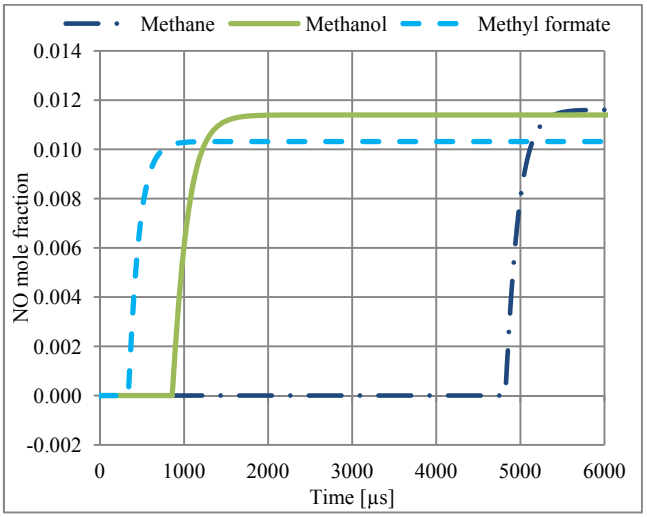

Fig. 12. NO concentration profiles for methane, methanol and methyl formate/air homogeneous mixtures at temperature of 1300 K and pressure of 2.7 atm

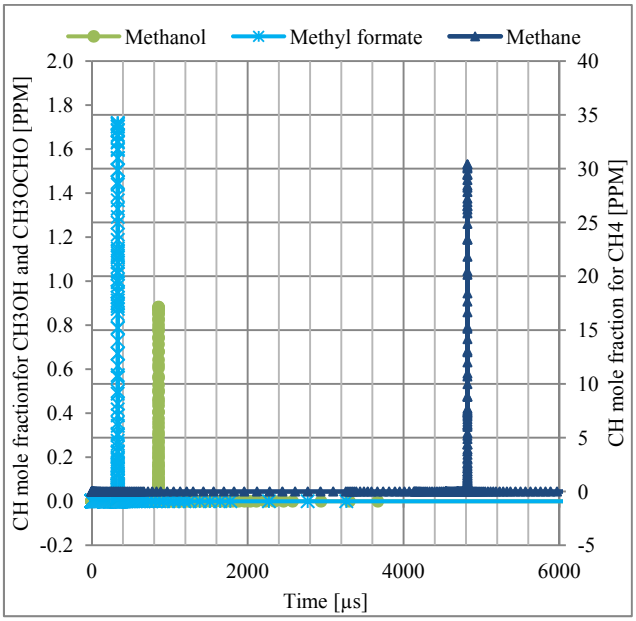

Fig. 13. CH concentration profiles for methane, methanol and methyl formate/air homogeneous mixtures at temperature of 1300 K and pressure of 2.7 atm

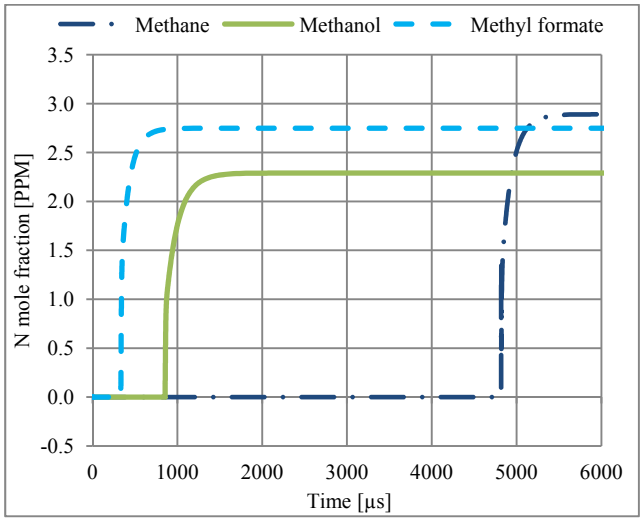

Fig. 14. N concentration profiles for methane, methanol and methyl formate/air homogeneous mixtures at temperature of 1300 K and pressure of 2.7 atm

V. Conclusion

Numerical simulations of NO production in CH_4, CH_3OH and CH_3OCHO under three different flame configurations: homogenous system; freely propagating flame; and diffusion flame; have been investigated.

It has been established that, under the different flow configurations considered, CH_4 has high amount of total NO present in the flame region as compared to the oxygenated fuels (CH_3OH and CH_3OCHO). The difference in the amount of NO produced by each fuel differ under different configurations. A significant difference (one order of magnitude higher) is observed in CH_4 under freely propagating and diffusion flames as compared to oxygenated fuels. In homogenous system the difference in the amount of NO produced by the three fuels is within the same order of magnitude. The NO formation in freely propagating and diffusion flames is mostly through prompt NO since the maximum flame temperatures attained are relatively low (approximately $\leq$ 2000 K). While the NO formation in a homogeneous system is mostly through thermal NO mechanism (Zel'dovich mechanism) since they attained high flame temperatures (approximately 2900 K) due to high initial temperatures.

Acknowledgment

The authors gratefully acknowledge the financial support of the Dedan Kimathi University of Technology, whose Combustion Simulation Laboratory Software package (COSILAB) was used to carry out the Flame simulations.

References

[1] S. C. Li and F. A. Williams, "NO_x formation in two-stage methane-air flames," *Combustion and Flame*, vol. 118, pp. 399–414, 1999.

[2] A. Bakali, L. Pillier, P. Desgroux, B. Lefort, L. Gasnot, J. F. Pauwels, and I. Da Costa, "NO prediction in natural gas flames using GFD-Kin^R 3.0 mechanism NCN and HCN contribution to prompt-NO formation," *Fuel*, 2006.

[3] A. A. Konnov, "Implementation of the NCN pathway of prompt-NO formation in the detailed reaction mechanism," *Combustion and Flame*, vol. 156, pp. 2093–2105, 2009.
[4] H. Guo, F. Liu, and G. J. Smallwood, "A numerical study of NO_x formation in laminar counterflow CH4 /air flames," *Combustion and Flame*, vol. 143, pp. 282–298, 2005.
[5] S. Naha and S. K. Aggarwal, "Fuel effects on NOx emissions in partially premixed flames," *Combustion and Flame*, vol. 139, pp. 90–105, 2004.
[6] E. C. Zabetta and M. Hupa, "A detailed chemical kinetic mechanism including methanol and nitrogen pollutants relevant to the gas-phase combustion and pyrolysis of biomass-derived fuels," *Combustion and Flame*, vol. 152, pp. 14–27, 2008.
[7] J. K. Tanui and P. N. Kioni, "The effect of fuel/air mixture composition on NO formation in methane, methanol and methyl formate freely propagating flames," in *Proceedings of 2012 Mechanical Engineering Conference on Sustainable Research and innovation,* 2012.
[8] J. K.Tanui and P. N. Kioni, "Numerical simulation of NO formation in methane, methanol and methyl formate in a homogeneous system," in *Proceedings of 2012 Mechanical Engineering Conference on Sustainable Research and innovation*,, 2012.
[9] S. Dooley, H. W. Sang, M. Chaos, J. Heyne, J. Yiguang, F. L. Dryer, K. Kumar, C. J. Sung, H. Wang, M. A. Oehlschlaeger, R. J. Santoro, and T. A. Litzinger, "A jet fuel surrogate formulated by real fuel properties," *Combustion and Flame*, vol. 157, 2010.
[10] E. M. Fisher, W. J. Pitz, H. J. Curran, and C. K. Westbrook, "Detailed chemical kinetic mechanisms for combustion of oxygenated fuels," in *Proceedings of the Combustion Institute*, 2000.
[11] C. K. Westbrook *et al.*, "A detailed chemical kinetic reaction mechanism for oxidation of four small a detailed chemical kinetic reaction mechanism for oxidation of four small alkyl esters in laminar premixed flames," *32nd International Symposium on Combustion Montreal, Canada,* 2008.
[12] P. A. Glaude, O. Herbinet, S. Bax, J. Biet, B. Valerie, and F. B. Lederc, "Modeling of the oxidation of methyl esters validation for methyl hexanoate, methyl heptanoate and methyl decanoate in a jet stirred reactor," *Combustion and Flame,* vol. 157, pp. 2035–2050, 2010.
[13] O. Herbinet, W. J. Pitz, and C. K. Westbrook, "Detailed chemical kinetic mechanism for the oxidation of biodiesel fuels blend surrogate," *Combustion and Flame*, 2009.
[14] C. V. Naik, C. K. Westbrook, O. Herbinet, W. J. Pitz, and M. Mehl, "Detailed chemical kinetic reaction mechanism for biodiesel components methyl stearate and methyl oleate," *The 33rd International Symposium on Combustion Beijing, China*, 2010.
[15] C. K. Westbrook, C. K. Naik, O. Herbinet, W. J. Pitz, M. Mehl, S. M. Sarathy, and H. J. Curran, "Detailed chemical kinetic reaction mechanisms for soy and rapeseed biodiesel fuels," *Combustion and Flame,* vol. 158, p. 742755, 2011.
[16] S. M. Sarathy, M. J. Thomson, W. J. Pitz, and T. Lu, "An experimental and kinetic modeling study of methyl decanoate combustion," *The 33rd International Symposium on Combustion Beijing, China*, 2010.
[17] I. G. Valeri and Y. Junfeng, "Construction of combustion models for rapeseed methyl ester bio-diesel fuel for internal combustion engine applications," *Biotechnology Advances*, 2009.
[18] G. P. Smith *et al.*, GRI Mech Version 3.0. [Online]. Available: http://www.me.berkeley.edu/grimech/ or, 1999
[19] S. Dooley *et al.*, "An experimental and kinetic modeling study of methyl formate oxidation," in *Proceedings of the European Combustion Meeting,* 2009.
[20] K. J. Hughes, T. Turanyi, M. J. Pilling, and A. S. Tomlin, Leeds NO_x mechanism. [Online]. Available: http://garfield.chem.elte.hu/Combustion/mechanisms/LeedsNOx20.dat 1999.
[21] R. S. Barlow, A. N. Karpetis, J. Frank, and J. Y. Chen, "Scalar profiles and NO formation in laminar opposed-flow partially premixed methane/air flames," *Combustion and Flame*, vol. 127, pp. 2102–2118, 2001.
[22] K. J. Hughes *et al.*, "An investigation of important gas-phase reactions of nitrogenous species from simulation of experimental measurements in combustion systems," *Combustion and Flame*, vol. 124, pp. 573–589, 2001.
[23] Rotexo, COSILAB Manual: 1-D and Counter-flow Flames including burner-stabilized & freely propagating flames, 2009.
[24] COSILAB, "Version 3, Rotexo-Cosilab gmbh & co. kg, bad zwischenahn, germany," www.rotexo.com, 2012.
[25] A. Burcat and B. Ruscic, "Third millennium ideal gas and condensed phase thermochemical database for combustion with updates from active thermochemical tables," *Argonne National Laboratory Report No. ANL-05/20 TAE 960*, 2005.

J. K. Tanui was born in Kericho, Kenya in 1985. He obtained his BSc. (Hons) in Mechanical Engineering from Jomo Kenyatta University of Agriculture And Technology (JKUAT), Nairobi, Kenya, in 2009. He is currently doing his Masters Degree in Mechanical Engineering (Specializing in Thermofluid Engineering) in JKUAT.

He is currently working as a tutorial fellow in Dedan Kimathi University of Technology (DKUT), Nyeri, Kenya. He is currently doing research on combustion properties and pollutant formations in biodiesel fuels. He is interested in specializing in combustion science.

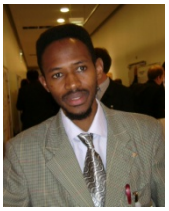

A. Gitahi was born in Nyeri, Kenya in 1973. He obtained his BSc. (Hons) in Mechanical Engineering from Jomo Kenyatta University of Agriculture and Technology (JKUAT), Nairobi, Kenya in 1998, and subsequently obtained his MSc. in Mechanical Engineering (thermofluids) from the same University in 2006.

He is currently working as a lecturer in the department of Mechanical Engineering at JKUAT. Subsequent to his Masters degree, he has done research work at Ruhr University-Bochum in Germany (2008-2009) involving lasers, as part of his ongoing PhD programme in CFD (with particular application to combustion in shear layers).

Mr Gitahi is a graduate member of both the Engineers Registration Board of Kenya (ERB) and the Institution of Engineers of Kenya (IEK).